THE ANATOLIAN JOURNAL OF CARDIOLOGY

Official journal of the TURKISH SOCIETY OF CARDIOLOGY

Desmosomal Junctions and Connexin-43 Remodeling in High-Pacing-Induced Heart Failure Dogs

ABSTRACT

Background: While desmosomal junctions and gap junction remodeling are among the arrhythmogenic substrates, the fate of desmosomal and gap junctions in high-pacing-induced heart failure remains unclear. This aim of this study was to determine the fate of desmosomal junctions in high-pacing-induced heart failure.

Methods: Dogs were randomly divided into 2 equal groups, a high-pacing-induced heart failure model group (heart failure group, n = 6) and a sham operation group (control group, n = 6). Echocardiography and cardiac electrophysiological examination were performed. Cardiac tissue was analyzed by immunofluorescence and transmission electron microscopy. The expression of desmoplakin and desmoglein-2 proteins was detected by western blot.

Results: A significant decrease in ejection fraction, significant cardiac dilatation, diastolic and systolic dysfunction, and ventricular thinning occurred after 4 weeks in high-pacing-induced dog model of heart failure. Effective refractory period action potential duration at 90% repolarization was prolonged in the heart failure group. Immunofluorescence analysis and transmission electron microscopy demonstrated connexin-43 lateralization accompanies desmoglein-2 and desmoplakin remodeling in the heart failure group. Western blotting showed that the expression of desmoplakin and desmoglein-2 proteins was higher in heart failure than in normal tissue.

Conclusion: Desmosome (desmoglein-2 and desmoplakin) redistribution and desmosome (desmoglein-2) overexpression accompanying connexin-43 lateralization were parts of a complex remodeling in high—pacing-induced heart failure.

Keywords: Connexin-43, desmosomes, gap junction, heart failure

INTRODUCTION

Arrhythmias caused by heart failure (HF) remain a major clinical problem for which a complete solution has not been found.[1] Therefore, the arrhythmogenic substrates affected by HF need to be further defined. Numerous studies have shown that arrhythmogenic substrates include myocardial hypertrophy, fibrosis, ischemia, myocardial electrical remodeling, and neuroendocrine regulation, as well as desmosomal and gap junction remodeling.[2-4]

Desmosomal and gap junctions are important components of intercellular connections and play a critical role in maintaining the structure and function of cardiac tissue.[5] These connections are concentrated at the intercalated disc (ID) between myocytes. Desmosomal junctions and gap junctions not only maintain the cytoskeleton but also participate in cell signaling and maintain synchronization within cell populations.[6] Both of them are key proteins in maintaining the electrical and mechanical stability of cardiac myocytes. It has been shown that remodeling of desmosome and gap junctions, involving changes in protein abundance and location, is the basis of severe arrhythmogenicity.[7-10] To date, the expression and remodeling of desmosomal junctions regarding HF models remain unstudied. Here, we used a dog model of high-pacing-induced HF to characterize gap junctions and desmosomal junctions to provide a basic background for understanding the arrhythmogenic substrate of HF.

ORIGINAL INVESTIGATION

Qing Wang[1,2#]
Xiaoyan Liang[1,2#]
Shuai Shang[1,2]
Yongqiang Fan[1,2]
Huasheng Lv[1,2]
Baopeng Tang[1,2]
Yanmei Lu[1,2]

[1]*Department of Pacing and Electrophysiology, The First Affiliated Hospital of Xinjiang Medical University, Xinjiang, China*
[2]*Xinjiang Key Laboratory of Cardiac Electrophysiology and Cardiac Remodeling, The First Affiliated Hospital of Xinjiang Medical University, Xinjiang, China*

Corresponding author:
Yanmei Lu
✉ 18909917855@189.cn

Received: November 26, 2022
Accepted: March 22, 2023
Available Online Date: May 5, 2023

Cite this article as: Wang Q, Liang X, Shang S, et al. Desmosomal junctions and connexin-43 remodeling in high-pacing-induced heart failure dogs. *Anatol J Cardiol.* 2023;27(8):462-471.

#Q.W. and X.L. contributed equally to this work.

DOI:10.14744/AnatolJCardiol.2023.2823

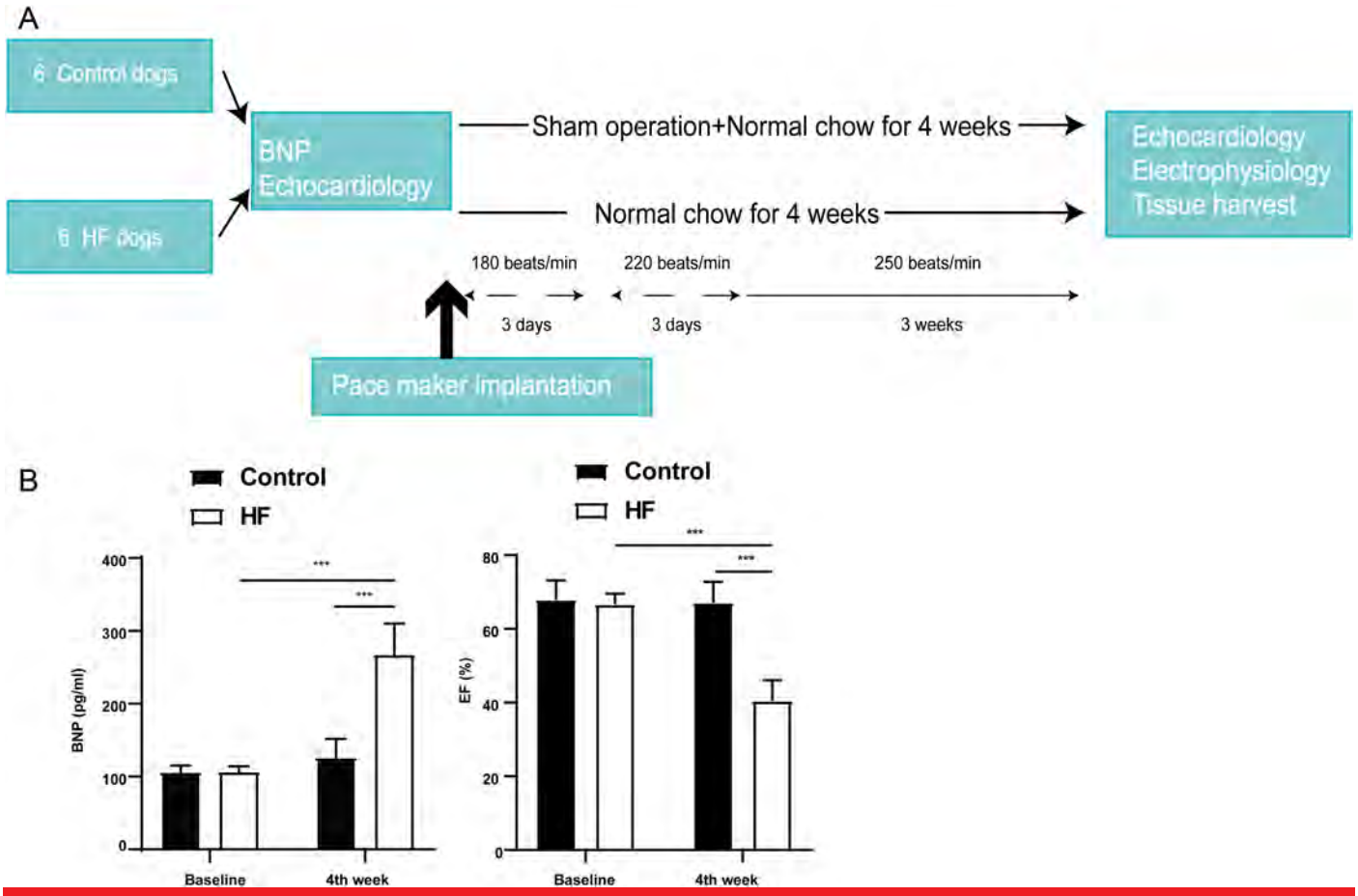

Figure 1. Flowchart and successful establishment of HF dogs. (A) Flowchart. (B) Level of plasma BNP and EF on the baseline and the fourth week. BNP, B-type natural peptide; HF, heart failure; EF, ejection function,* $P < .001$ vs. control, n = 6 for each group.**

METHODS

Construction of High-Pacing-Induced Heart Failure Dog Model

Twelve adult dogs (SPF) were randomly assigned to 2 equal groups (Figure 1A), a 4-week high-pacing-induced HF model (HF group, n = 6) and a sham operation group (control group, n = 6). A dog model of high-pacing-induced HF was implanted with a pacemaker in the right ventricle for 4 weeks, as described in our previous study.[11] Briefly, corkscrew electrodes are implanted in the apex of the right ventricle and connected to a pacemaker under general sterile conditions (Figure 1A, pacing frequencies: 180 beats/min, 3 days; 220 beats/min, 3 days; 250 beats/min, 3 weeks). The dogs were housed and bred under SPF conditions in the animal facility at Xinjiang Medical University. An ultrasound was performed preoperatively on all dogs, and serial echocardiography (baseline, fourth week) was used to determine their cardiac function (Figure 1A). Dogs were euthanized before tissue collection. Sirius red staining was performed to evaluate myocardial fibrosis. The ImageJ software was used to quantify the positive areas. Blood plasma samples were subjected to ELISA (enzyme linked immunosorbent assay) testing to determine the concentration of BNP (Jianglai, China). All dogs were used in compliance with the Declaration of Helsinki.

Electrophysiology

The electrophysiological examination of 2 groups was conducted after 4 weeks to observe the incidence of ventricular fibrillation. The electrophysiological detection method was as follows: first, 3 electrodes were connected to the dog's body surface to monitor the electrocardiogram on the body surface. Second, the lead was implanted into the left ventricular apex through the internal jugular vein. Then, 2 groups were subjected to programmed electrical stimulation [pacing was started with twice as much as the threshold, 8

HIGHLIGHTS

- The incidence of ventricular arrhythmia is significantly increased in high-pacing-induced heart failure (HF) dogs.
- Connexin-43 lateralization was found in high-pacing-induced HF.
- Desmosome remodeling in a new location: similar to connexin-43 lateralization, desmosome junctions were distributed parallel to the myocardial fibers in high-pacing-induced HF. Further, desmosome protein desmoglein-2 overexpression in HF is one of the potential factors of myocardial remodeling.

times stimulation, the cycle length was 140 ms (S1); additional stimulation (S2) was applied] to observe the incidence of ventricular fibrillation.

The effective refractory period (ERP) of the ventricles was detected as follows: multi-electrode catheters were sutured to the left and right ventricles. All dogs received programmed stimulation with the LEAD-7000 system. Effective refractory period was measured as described in our previous study.[12] Briefly, ERPs were calculated at 8 basic cycle lengths of 320 ms, followed by premature ventricular stimulation (S2) in 5 ms decrements until S2 failed to capture depolarization. The longest S1-S2 interval that did not elicit a propagating response at each site was defined as the ERP.

In addition, a bipolar custom-made Ag-AgCl catheter was placed in the outer membrane of the ventricle to record the action potential duration (APD) in the ventricle during a 1-minute stable observation. Action potential duration of 90% repolarization was defined as the duration of 90% repolarization, and 4-5 consecutive APD_{90} values were measured and averaged.

Echocardiography

Echocardiography was performed in a conscious state by Philips Ultrasound (Sonos5500, United States) as in our previous study.[11] The parameters were recorded at baseline and the fourth week as follows: left atrium (LA); right atrium (RA); right ventricular end-diastolic diameter (RV); left ventricular end-diastolic diameter (LVDd); left ventricular end-systolic diameter (LVDs); left ventricular posterior wall in diastole (LVPWd); left ventricular posterior wall in systole (LVPWs); and left ventricular ejection fraction (EF).

Immunofluorescence

Colocalization of connexin-43 (Cx43) with desmoglein-2 (DSG2) and desmoplakin (DP) was assessed by immunofluorescence in ventricular tissue of control and HF groups. The paraffin section of cardiac tissue was dewaxed to water, and the tissue section was placed in a repair box filled with antigen repair buffer solution (PH8.0) for antigen repair in the microwave oven. The antigen was sealed with hydrogen peroxide, and BSA was added for 30 minutes. Then paraffin sections were incubated with the primary antibody [anti-Cx43 (ab11370, 1:400, Abcam, Cambridge, MA, USA), anti-DSG2 (bs-10152R, 1:200, Bioss, Beijing, China), and anti-DP (bs-1748R, 1:200, Bioss)] for 1 hour. These sections were washed with PBS and incubated with a secondary antibody.

As with the previous studies, the "plaque" was defined as a more contiguous immunoreactive signal.[13] Most plaques' long axis is oriented either parallel or perpendicular to the cardiac fibers, while other plaques were considered as "undefined" because it did not have a well-defined long axes (corresponding to circular or irregularly shaped plaques). Plaques were counted to determine the lateralization rate of proteins (i.e., the proportion of plaques with a long axis parallel to the cardiac fiber direction) in 2 groups. Connexin-43 colocalization with DSG2 or DP was determined by the Pearson's correlation coefficient.

Transmission Electron Microscope

Desmosomes and gap junctions between myocardial cells were identified by transmission electron microscopy (JEM-1230, JEOL Ltd, Japan). The cardiac tissue was fixed with 4% glutaraldehyde for 24 hours and dehydrated in a graded ethanol series. After dehydration, myocardial tissue was fixed with 0.5% osmium tetroxide and finally embedded in epoxy resin.[14]

Western Blot

Cardiac tissue was homogenized in RIPA buffer. Protein concentration was determined using Bio-Rad Bradford reagent. Equal amounts of protein (20 μg) were loaded onto a 10% SDS/polyacrylamide gel. Proteins were transferred to nitrocellulose membrane and blocked with 5% skimmed milk. Membranes were incubated with primary antibodies [anti-Cx43 (ab11370, 1:1000, Abcam, USA), anti-DSG2 (bs-10152R, 1:1000, Bioss), GAPDH (Glyceraldehyde-3-phosphate dehydrogenase) (MAB374, 1:2000, Chemicon, USA)] overnight at 4°C followed by secondary antibodies (1:5000, Zhongshanjinqiao, China) at room temperature for 1 hour. Immunodetection of bands was revealed by ECL Plus solution (GE Healthcare, USA). The bands were quantified by ImageJ and were normalized to GAPDH.

Quantitative Reverse-Transcription Polymerase Chain Reaction

Reverse-transcription polymerase chain reaction (RT-qPCR) was performed to quantify the mRNA expression levels of Cx43, DSG2. Total RNA was extracted with TRIzol reagent (Life Technologies, USA), according to the instructions of the manufacturer. Reverse transcriptase (Thermo Fisher Scientific, USA) was used for reverse transcription, and RT-qPCR was performed using a Quantitect SYBR Green PCR Kit (Qiagen, Germany) in a 7500 RT-qPCR System (Applied Biosystems, Foster City, CA, USA) using 7500 software (Version 2.3). GAPDH was used as an internal reference. The quantitative expression results were calculated using the $2^{-\Delta\Delta Ct}$ method. All primer sequences of tested genes are presented in Table 1.

Statistical Analysis

Continuous values were represented as mean ± SD. Continuous variables between 2 groups that conform to the normal distribution are detected by Student's *t*-test, otherwise Mann–Whitney *U*-test was used if the data did not accord with normal distribution. Categorical values were presented as numbers and percentages. To compare

Table 1. The Primers Used in this Study

Genes	Primers
GAPDH	F: 5′-GCAAATTCCACGGCACAGTCAAG-3′
	R: 5′-ACAACATACTCAGCACCAGCATCAC-3′
Cx43	F: 5′-TCTGCTATGACAAATCCTTCCCA-3′
	R: 5′-CTCCTCCTCTTTCTTGTTCAGTTTCT-3′
DSG2	F: 5′- GCTCTGCCCTCATCAAAGACCATC-3′
	R: 5′- GCTCCTGTTGTTCCTGTCACTTGG-3′

Cx43, connexin-43; DSG2, desmoglein-2.

the number of ventricular fibrillation by burst stimulation, Fisher's exact test was applied. Statistical Package for Social Sciences 22.0 software was used for data analysis, $P < .05$ was defined as statistical significance.

RESULTS

Generation of the High-Pacing-Induced Heart Failure Model

Before the cardiac pacemaker surgery, echocardiography showed normal cardiac morphology, dimensions, and motion in HF group (Figure 1A). Compared with baseline, EF was decreased in the fourth week in the HF group ($P < .001$, Figure 1B). Further, plasma BNP was significantly increased in the fourth week in the HF group compared with baseline ($P < .001$, Figure 1B). Compared with the control group, plasma BNP was decreased in the HF group ($P < .001$, Figure 1B). Echocardiography measurements indicated a significant reduction in EF, LVPWd, and LVPW of HF group relative to controls ($P < .001$, Figure 2A and B), whereas the RA ($P < .001$), LA ($P < .001$), RV ($P < .01$), LVDd ($P < .001$), and LVDs ($P < .001$) were significantly enlarged, compared to the control group (Figure 2B). Sirius red staining revealed markedly collagen deposition in the HF group compared with the control group ($P < .001$, Figure 2C and D).

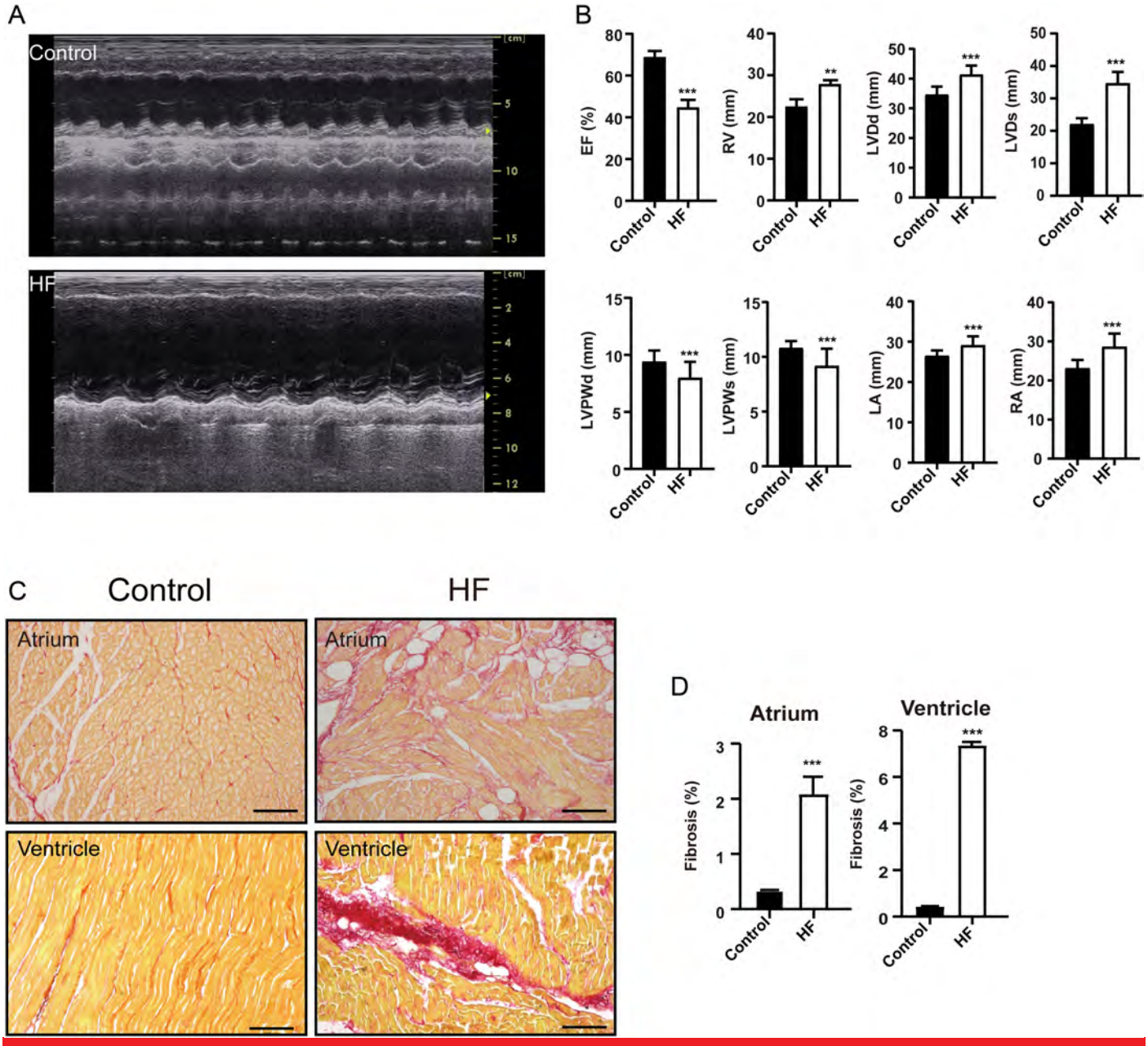

Figure 2. Echocardiography and cardiac fibrosis in HF dogs. (A) Representative echocardiography image in HF and control groups. (B) The echocardiography on the fourth week of HF. EF, ejection fraction; HF, heart failure; $^{**}P < .01$ vs. control, $^{***}P < .001$ vs. control. (C, D) Sirius scarlet staining ventricle in the control and HF group. HF, heart failure. $^{**}P < .01$ vs. control, $^{***}P < .001$ vs. control, n = 6 for each group, Bar = 100 μm.

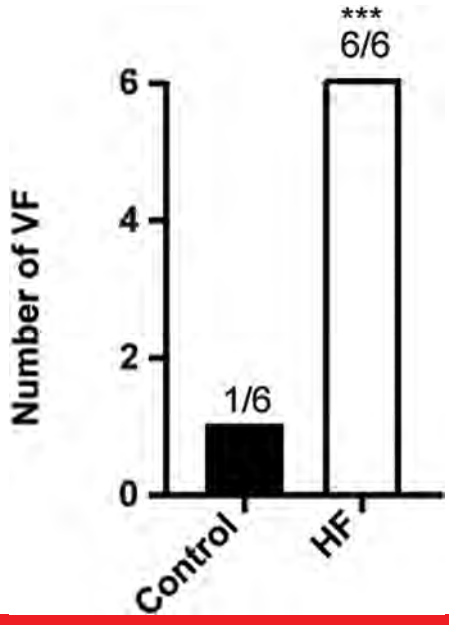

Figure 3. Incidence of ventricular fibrillation was increased in high-pacing-induced heart failure. Number of VF in control and HF groups through burst stimulation. HF, heart failure; VF, ventricular fibrillation. ***$P < .001$ vs. control, n = 6 for each group.

The number of ventricular fibrillation in the HF group was increased by the burst stimulation test (Figure 3). These results suggested that we had successfully created an animal model of HF, these HF dogs were susceptible to develop ventricular arrhythmias.

Electrical Remodeling in High-Pacing-Induced Heart Failure Dogs

After 4 weeks of rapid pacing, right ventricular ERP and APD_{90} were significantly prolonged in the HF model group compared with the control group (left ventricular ERP, 160 ± 33.01 vs. 164.17 ± 5.85, $P = .927$; right ventricular ERP, 183.33 ± 23.17 vs. 151.67 ± 12.11, $P < .01$; APD_{90}, 375.05 ± 17.29 vs. 249.04 ± 19.93 ms, $P < .001$).

Gap Junction Connexin-43Remodeling in High-Pacing-Induced Heart Failure Dogs

In the control group, the Cx43 signal is mainly perpendicular to the direction of the cardiac fiber (corresponding to ID) (Figure 4A and B). In contrast, signals parallel to fibers were found in HF group (Figure 4A and B). The Cx43 signal further showed that 10 plaques were considered perpendicular (accounting for 65% of the total of the 16 plaques), only 2 plaques were found to be parallel to the direction of cardiac fibers, and 4 were classified as "undefined" (Figure 4A and B). Nineteen plaques in the HF group were analyzed. There are almost no plaques perpendicular to the cardiac fiber orientation, 15 plaques are parallel to the fiber orientation, and 4 plaques are undefined (Figure 4A and B). Consistent with previous studies, plaques in vertical or parallel directions will be referred to as "ID" or "LM" (lateral membranes), respectively.[13] These results indicate that Cx43 has undergone extensive remodeling in this HF, and Cx43 plaques parallel to the fiber axis are dominant.

Desmosomal Junctions Remodeling in High-Pacing-Induced Heart Failure Dogs

Immunostaining showed that DSG2 plaques had a similar pattern to Cx43 plaques in the control group (Figure 4A and C). Twelve plaques of DSG2 were analyzed in the control group, 5 plaques were identified as vertical (42%), 4 (33%) undefined, and 3 (25%) parallel (Figure 4A and B). In HF group, 89% of plaques (12 total) were parallel (Figure 4A and C). Desmoplakin plaques were rarely seen in control tissue, but DP plaques (90%) were parallel to cardiac fibers. The signal overlay showed that Cx43 and DSG2/DP colocalize to the same cellular region. Magnified images of plaques formed at the LM showed a characteristic pattern of desmosomes and Cx43 colocalization, with overlapping or alternating pixels showing positive for one or the other protein (Figure 4A; panels a, b, c, d, and e; and D). This study further suggests that the lateralization of Cx43 is not an isolated event. A complex remodeling process including the remodeling of gap and desmosome junctions occurs in the cardiac cells of HF.

A more direct demonstration of gap and desmosomes lateralization was obtained by transmission electron microscopy (Figure 5). The image in low-resolution Figure 5A shows the cardiac fiber orientation of the right ventricle in the HF group. The enlargement of the area delineated by the red box corresponds to the lateral gap and desmosomes of cardiomyocytes, as shown in Figure 5B. These results provide evidence that gap and desmosomes structures can be formed at the LM of cardiomyocytes.

Desmosomes Proteins and Connexin-43 Overexpression in the Right Ventricle of High-Pacing-Induced Heart Failure

Western blot analysis and qRT-PCR characterized the expression of desmosomes proteins and gap junction Cx43. The study found that DSG2, DP, and Cx43 were overexpressed in myocardium of HF compared with the control group (Figures 6 and 7). It is further suggested that desmosome remodeling of HF not only includes changes in location but also changes in protein abundance.

DISCUSSION

Main Findings

Arrhythmias have long been recognized as part of the clinical presentation of HF. Given the variety of arrhythmias, understanding the arrhythmia mechanism behind HF is necessary to treat it. For this reason, the main arrhythmogenic substrate of HF was investigated in this study. This study showed that significant structural remodeling and electrical remodeling of the myocardium occurred in a dog model of high-pacing-induced HF. The incidence of ventricular arrhythmias was significantly increased in this class of HF models. Most importantly, gap junctions and desmosome remodeling are important components of the arrhythmogenic substrate. In this study, lateralized remodeling and overexpression of desmosome junctions accompanied by gap junction remodeling were found in high-pacing-induced HF.

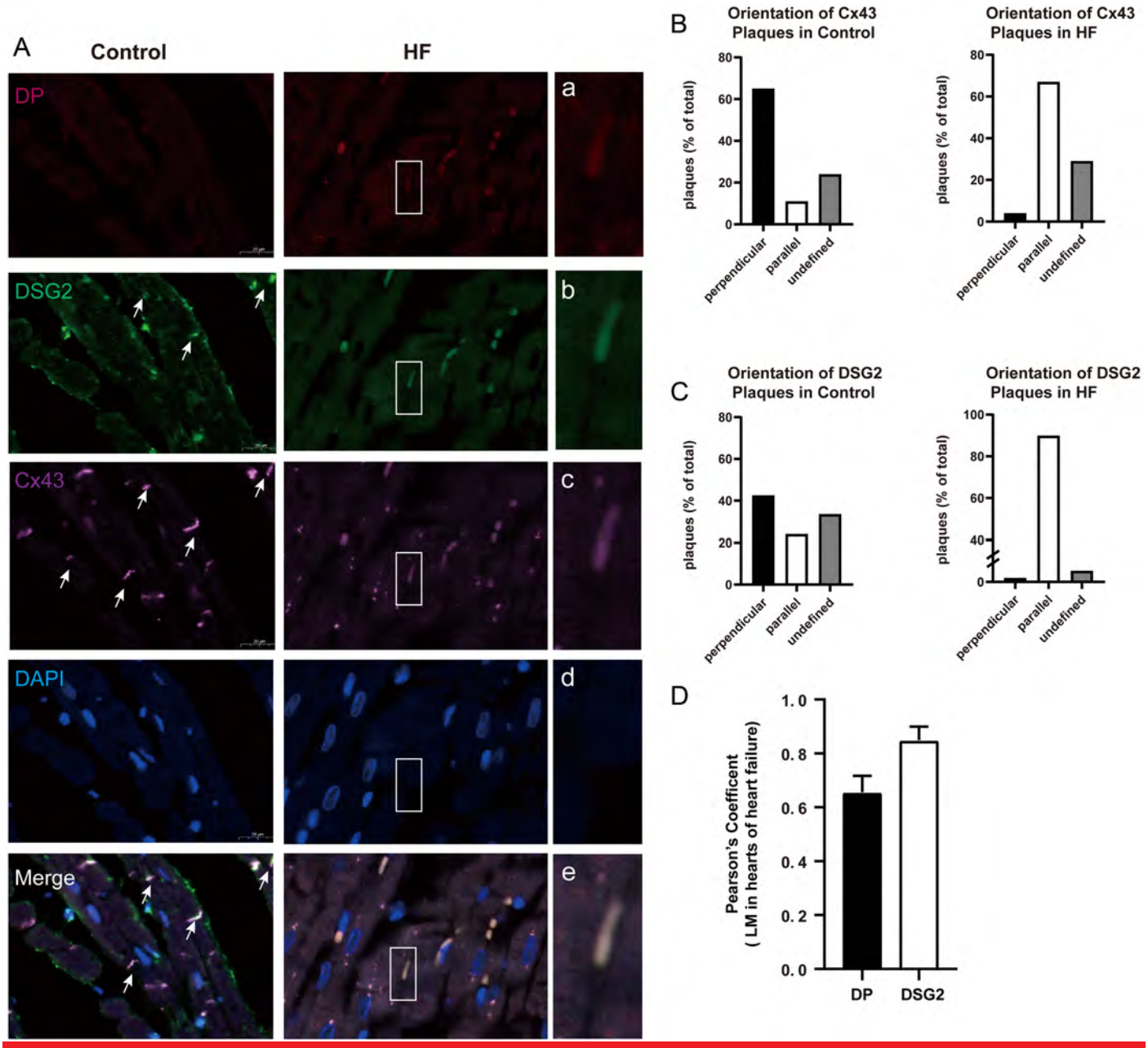

Figure 4. Immunofluorescent staining for the DP, DSG2, and Cx43. (A) Representative immunofluorescent images of DP, DSG2, and Cx43 in the myocardial. (B) Cx43 and DSG2 distribution. (C) Comparison of Pearson coefficient values for colocalization of Cx43 with various molecules (DSG2, DP) at the LM in the hearts of HF group. Cx43, Connexin-43; DP, Desmoplakin; DSG2, desmoglein-2; HF, heart failure; LM, lateral membrane.

Myocardial Structural Remodeling in High-Pacing-Induced Heart Failure

Supraventricular or ventricular tachyarrhythmias trigger tachycardia cardiomyopathy, which can eventually lead to HF.[15,16] The HF model established by rapid pacing for 4 weeks used in this study is a typical tachycardia cardiomyopathy-induced HF animal model. The high-pacing-induced HF model has been used for more than 60 years. The model is similar to human dilated cardiomyopathy in hemodynamic and structural aspects. In this model, typical manifestations of HF include ascites, pulmonary edema, decreased cardiac output, and elevated RA, pulmonary capillary wedge, and left ventricular end-diastolic pressure.[17-20] Previous studies have reported that exposure to a high-pacing-induced HF model results in left ventricular systolic/dilatation dysfunction, biventricular dilation with mild thinning or without associated hypertrophy.[21] In contrast, cardiac output, EF, and cardiac volume continued to deteriorate over the next 4 weeks. Our work proved similar results which are a significant decrease in EF, significant cardiac dilatation, diastolic and systolic dysfunction, and ventricular thinning occurred after 4 weeks in high-pacing-induced dog model of HF. This is because rapid ventricular pacing inevitably leads to myocardial asynchrony, resulting in faster ventricular contractile

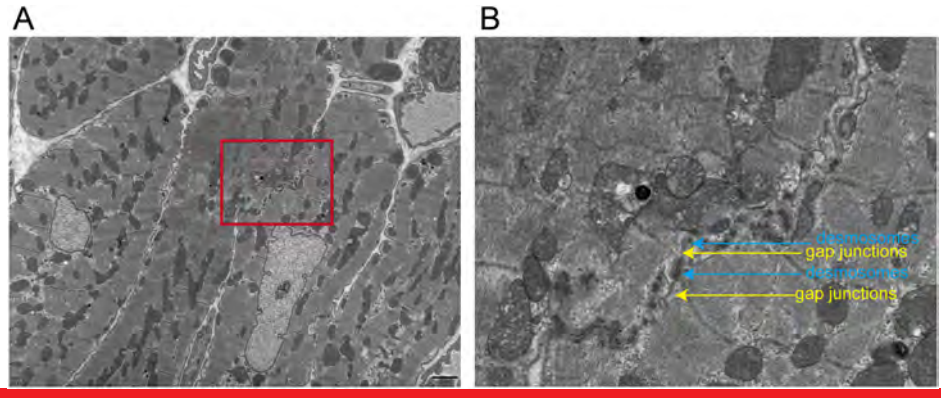

Figure 5. Electron microscopy image obtained from the right ventricle of a high-pacing-induced dog. (A) Low-magnification image (=2600×) shows preservation of structures and orientation of cardiomyocytes. (B) Area within the red square in A is shown in B at higher magnification picture. Notice the presence of lateralized desmosomes (blue arrow) and gap junctions (yellow arrow) oriented parallel to fiber direction.

performance and subsequent dramatic decline, ultimately leading to structural remodeling.

The rapidly paced dog model of HF exhibited myocardial fibrosis after 4 weeks. Myocardial fibrosis is caused by increased myofibroblast activity and extracellular matrix protein deposition, which can contribute to arrhythmias via a reentrant mechanism.[22] Consistent with previous findings, dogs with high-pacing-induced HF had massive extracellular matrix collagen deposition. A previous study showed that the fibrotic areas are intertwined with the cardiomyocytes and promote slow conduction, which in turn causes reentrant ventricular tachycardia.[23] Thus, fibrosis of the myocardium is one of the arrhythmogenic substrates in rapid pacing-induced HF.

Electrical Remodeling in High-Pacing-Induced Heart Failure

The electrophysiology of failing cardiomyocytes has been extensively studied in various HF animal models.[24] Electrophysiological changes or adverse electrical remodeling in HF include prolongation of APD, reduced conduction velocity, disturbed excitation–contraction coupling, and the changes of ERP.[25,26] Moreover, APD prolongation has been consistently observed in various HF animal models.[27-29]

Consistent with previous studies, in the dog model of high-pacing-induced HF, the APD_{90} of cardiomyocytes was prolonged. Further, the ERP was prolonged in high-pacing-induced HF model. Both APD and ERP prolongation affect ventricular arrhythmia development. On the one hand, the prolongation of the ERP creates arrhythmic substrates for the onset and perpetuation of ventricular arrhythmias.[30] On the other hand, prolonged APD alters the refractory period and elicits arrhythmias.[31] Prolonged APD in turn promotes ERP prolongation and leads to an increased propensity for ventricular arrhythmias.[32] In sum, our current study suggests significant electrical remodeling as well as a significant increase in the incidence of ventricular arrhythmias in high-pacing-induced HF.

Gap Junctions Remodeling in High-Pacing-Induced Heart Failure

At the cellular and molecular level, electrophysiological alterations in the failing heart also involve intercellular gap junctions. Heterogeneous changes in the expression, distribution, and density of gap junctions play a role in the pathogenesis of ventricular arrhythmias.[33] Gap junctions are specialized membrane channels composed of protein

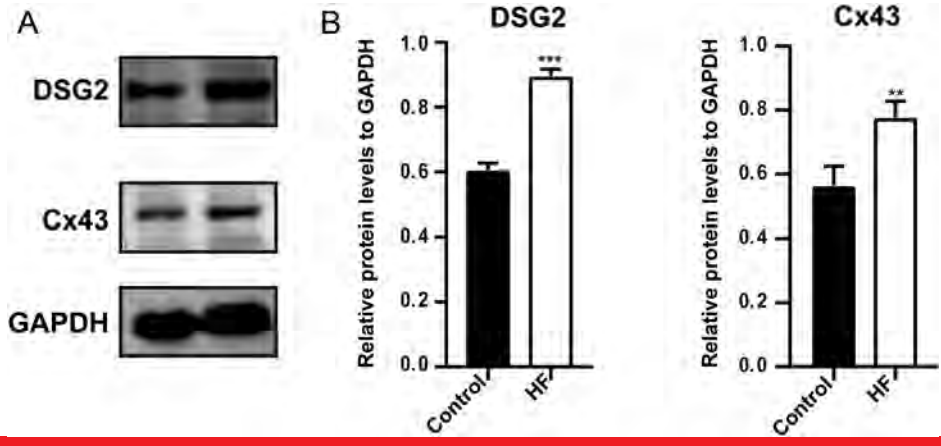

Figure 6. Relative protein expression of DSG2, Cx43. Cx43, DSG2 protein expression by western blot. Cx43, Connexin-43; DSG2, desmoglein-2. $^{**}P < .01$ vs. control, $^{***}P < .001$ vs. control, n = 6 for each group.

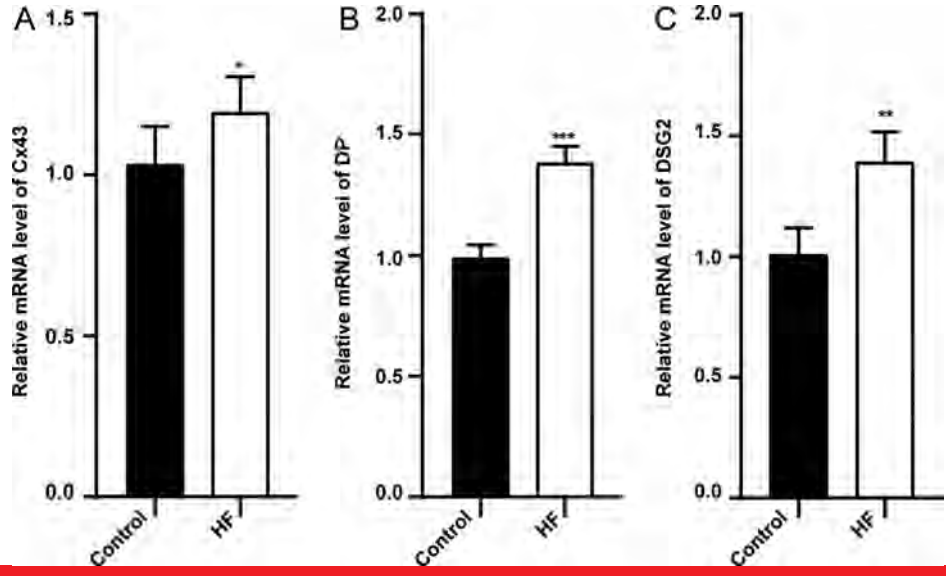

Figure 7. Relative mRNA expression of DSG2, Cx43 by qRT-PCR. $^{*}P < .05$ **vs. control,** $^{**}P < .01$ **vs. control,** $^{***}P < .001$ **vs. control, n = 6 for each group.**

subunits called connexins.[34] It provides the basis for mediating electrical and chemical communication between neighboring cardiomyocytes.[35-37]

Cardiomyocytes are composed of 3 major connexins, mainly connexin (Cx) 43, Cx40, and Cx45.[38] Connexin-43 is the most abundant gap junction protein in the cardiovascular system.[39] For this reason, the present study further observed Cx43 and expression and distribution in high-pacing-induced HF. Consistent with previous studies, in the normal heart, Cx43 is mainly present at the end-to-end junctions or insertion discs of cells. In contrast, the Cx43 in rapidly paced HF is redistributed from the ID to the borders of the whole cell (parallel to the fiber direction). The phenomenon of parallel to the fiber direction is defined as Cx43 lateralization.[40] Electron microscopic images were obtained to characterize the microstructure of cardiomyocytes: both gap junctions and desmosome junctions are distributed laterally in the cardiomyocyte. Cx43 lateralization has been reported in a variety of HF models, such as ischemic, congestive HF, and end-stage HF.[41-44] The lateralized distribution of Cx43 protein in cardiomyocytes affects intercellular coupling as well as the direction of electrical conduction in the heart (zig-zag conduction), thus promoting arrhythmias.[45]

In terms of the expression of Cx43 molecules in HF, previous studies have reported a 50% reduction in Cx43 expression in HF. Decreased Cx43 expression contributes to the uncoupling of gap junctions, therefore causing conduction slowing heterogeneities and facilitating arrhythmias.[46] Unlike previous studies, the present study found a significant increase in Cx43 expression. Previous studies have reported that Cx43 expression has also been shown to be heterogeneous, with expression appearing to vary in different regions of the heart.[47] Thus, Cx43 expression may be associated with the different experimental designs and the different target regions of the heart.

Desmosome Junctions Remodeling in High-Pacing-Induced Heart Failure

In addition, desmosome junctions also relate to electrophysiological alterations and cardiac remodeling. Desmosome junctions are an important component of intercellular junctions and are used to maintain electromechanical stability between cardiac myocytes.[48] Mutations and abnormal expression of desmosomal genes have been shown to cause arrhythmias.[49] Prevention or reversal of desmosomal remodeling provides a strategy to repair damaged hearts. Therefore, there is an urgent need to reveal the fate of desmosome junctions in HF.

We characterized the morphology and protein expression of desmosome junctions using a dog model of high-pacing-induced HF. It was found that desmosome junctions were distributed parallel to myocardial fibers in high-pacing-induced HF model, similar to Cx43 lateralization. These data suggest an interconnection between desmosome and Cx43. In addition, previous studies have found that at the embryonic stage, desmosome forms new intercellular junctions before the gap junction protein Cx43.[12,50] The disruption of desmosome directly leads to rearrangement of Cx43 distribution, resulting in Cx43 lateralization. It further suggests a close relationship between desmosome and Cx43 distribution. Not only that, Chkourko et al[13] found desmosome lateralized distribution of cardiomyocytes in a model of pressure overload-induced pulmonary hypertension. This further suggests that the distribution of desmosome junctions parallel to the direction of myocardial fibrosis may be present in a variety of cardiovascular diseases. However, it is still unclear whether the abnormal distribution of desmosome junctions is involved in intercellular coupling or cardiac electrical conduction in HF. Further analysis of the electrophysiological changes resulting from the abnormal distribution of desmosome junctions is needed in the future.

To date, only 2 studies in cardiovascular disease have investigated the abundance of desmosome protein expression. A study found that DSG2 and DSC were significantly increased in patients with dilated cardiomyopathy and ischemic cardiomyopathy.[51] Another study showed that desmosomal proteins plakoglobin was significantly increased in a model of pulmonary hypertension.[13] Unlike previous studies, our study focuses on the abundance of desmosome protein expression in high-pacing-induced HF. Taking the typical desmosome protein-DSG2 protein as an example, our study found a significant increase in the expression of myocardial DSG2 in dogs with high-pacing-induced HF. Desmoglein-2 is a transmembrane desmosomal cadherin. It is essential for cardiomyocyte cohesion and barrier function to maintain the mechanical stability of the heart. Combined with previous studies, we found that desmosome protein overexpression is popular in cardiovascular diseases. The pathophysiology of the rapid pacing-induced HF model differs from that of ischemic HF and dilated HF, so further clarify the abundance of DSG2 expression in ischemic HF and dilated HF is needed.

A growing number of studies have identified a variety of molecular functions of desmosome proteins. In humans, mutations in desmosomal proteins (usually DSG2, DP, DSC, PKP, etc.) lead to arrhythmias. Overexpression of desmosomal protein DSC leads to myocardial fibrosis and remodeling of a rat.[52,53] These results suggest a link between desmosome protein molecular function and myocardial remodeling/electrical remodeling. Clarification of the relationship between DSG2 overexpression and electrical remodeling seems to facilitate our understanding of arrhythmogenic substrates in HF.

Study Limitations

This study has several limitations. First, this study still cannot answer whether the distribution of desmosomes parallel to the myocardium affects the cardiac conduction in HF. Second, the relationship between desmosome overexpression and electrical remodeling in HF has not been found.

CONCLUSION

In conclusion, desmosome redistribution and overexpression accompanying gap junction Cx43 remodeling were found in HF.

Data Availability Statement: The datasets were available.

Ethics Statement: All dogs were used in compliance with the Declaration of Helsinki. The Ethics Committee of the First Affiliated Hospital of Xinjiang Medical University approved this study (approved number: IACUC-201902-K03; approved date: 2021.5.3).

Peer-review: Externally peer-reviewed.

Author Contributions: Data curation – W.Q., L.X., S.S., F.Y., T.B.; Formal analysis – W.Q., L.X.; Funding acquisition – L.Y.; Investigation – W.Q., L.X., L.H., L.Y.; Project administration – T.B.; Writing –original draft – W.Q., L.X.; Writing–review and editing – Z.X., T.B., L.Y.

Declaration of Interests: The authors declare that they have no conflicts of interest.

Funding: This work was funded by the National Natural Science Foundation of China (approved number: 81860081) and Top young scientific and technological talents of Tianshan Talent Cultivation Program in Xinjiang (2022TSYCCX0101).

REFERENCES

1. Alenazy B, Tharkar S, Kashour T, Alhabib KF, Alfaleh H, Hersi A. In-hospital ventricular arrhythmia in heart failure patients: 7 year follow-up of the multi-centric HEARTS registry. *ESC Heart Fail*. 2019;6(6):1283-1290. [CrossRef]
2. Ma S, Ma J, Mai X, Zhao X, Guo L, Zhang M. Danqi soft capsule prevents infarct border zone remodelling and reduces susceptibility to ventricular arrhythmias in post-myocardial infarction rats. *J Cell Mol Med*. 2019;23(8):5454-5465. [CrossRef]
3. Cicchitti V, Radico F, Bianco F, Gallina S, Tonti G, De Caterina R. Heart failure due to right ventricular apical pacing: the importance of flow patterns. *Europace*. 2016;18(11):1679-1688. [CrossRef]
4. Alvarez CK, Cronin E, Baker WL, Kluger J. Heart failure as a substrate and trigger for ventricular tachycardia. *J Interv Card Electrophysiol*. 2019;56(3):229-247. [CrossRef]
5. Pilichou K, Remme CA, Basso C, et al. Myocyte necrosis underlies progressive myocardial dystrophy in mouse dsg2-related arrhythmogenic right ventricular cardiomyopathy. *J Exp Med*. 2009;206(8):1787-1802. [CrossRef]
6. Zhao G, Qiu Y, Zhang HM, Yang D. Intercalated discs: cellular adhesion and signaling in heart health and diseases. *Heart Fail Rev*. 2019;24(1):115-132. [CrossRef]
7. Yan J, Killingsworth C, Walcott G, et al. Molecular remodeling of Cx43, but not structural remodeling, promotes arrhythmias in an arrhythmogenic canine model of nonischemic heart failure. *J Mol Cell Cardiol*. 2021;158:72-81. [CrossRef]
8. Boulaksil M, Winckels SKG, Engelen MA, et al. Heterogeneous connexin43 distribution in heart failure is associated with dispersed conduction and enhanced susceptibility to ventricular arrhythmias. *Eur J Heart Fail*. 2010;12(9):913-921. [CrossRef]
9. Ntalla I, Weng LC, Cartwright JH, et al. Multi-ancestry GWAS of the electrocardiographic PR interval identifies 202 loci underlying cardiac conduction. *Nat Commun*. 2020;11(1):2542. [CrossRef]
10. Zhu Y, Shamblin I, Rodriguez E, et al. Progressive cardiac arrhythmias and ECG abnormalities in the Huntington's disease BACHD mouse model. *Hum Mol Genet*. 2020;29(3):369-381. [CrossRef]
11. Liang X, Bai Z, Wang F, et al. Full-length transcriptome sequencing: an insight into the dog model of heart failure. *Front Cardiovasc Med*. 2021;8:712797. [CrossRef]
12 Corrado D, Link MS, Calkins H. Arrhythmogenic right ventricular cardiomyopathy. *N Engl J Med*. 2017;376(1):61-72. [CrossRef]
13. Chkourko HS, Guerrero-Serna G, Lin X, et al. Remodeling of mechanical junctions and of microtubule-associated proteins accompany cardiac connexin43 lateralization. *Heart Rhythm*. 2012;9(7):1133-1140.e6. [CrossRef]
14. Wang Z, Liang X, Lu Y, et al. Insomnia promotes hepatic steatosis in rats possibly by mediating sympathetic overactivation. *Front Physiol*. 2021;12:734009. [CrossRef]
15. Khurshid S, Frankel DS. Pacing-induced cardiomyopathy. *Card Electrophysiol Clin*. 2021;13(4):741-753. [CrossRef]
16. Ellis ER, Josephson ME. Heart failure and tachycardia-induced cardiomyopathy. *Curr Heart Fail Rep*. 2013;10(4):296-306. [CrossRef]
17. Solomon SB, Nikolic SD, Glantz SA, Yellin EL. Left ventricular diastolic function of remodeled myocardium in dogs with pacing-induced heart failure. *Am J Physiol*. 1998;274(3):H945-H954. [CrossRef]

18. Eising GP, Hammond HK, Helmer GA, Gilpin E, Ross J Jr. Force-frequency relations during heart failure in pigs. *Am J Physiol*. 1994;267(6 Pt 2):H2516-H2522. [CrossRef]
19. Travill CM, Williams TD, Pate P, et al. Haemodynamic and neurohumoral response in heart failure produced by rapid ventricular pacing. *Cardiovasc Res*. 1992;26(8):783-790. [CrossRef]
20. Marzo KP, Frey MJ, Wilson JR, et al. Beta-adrenergic receptor-G protein-adenylate cyclase complex in experimental canine congestive heart failure produced by rapid ventricular pacing. *Circ Res*. 1991;69(6):1546-1556.[CrossRef]
21. Gupta S, Figueredo VM. Tachycardia mediated cardiomyopathy: pathophysiology, mechanisms, clinical features and management. *Int J Cardiol*. 2014;172(1):40-46. [CrossRef]
22. Pilling D, Vakil V, Cox N, Gomer RH. TNF-α-stimulated fibroblasts secrete lumican to promote fibrocyte differentiation. *Proc Natl Acad Sci U S A*. 2015;112(38):11929-11934. [CrossRef]
23. Handa BS, Li X, Baxan N, et al. Ventricular fibrillation mechanism and global fibrillatory organization are determined by gap junction coupling and fibrosis pattern. *Cardiovasc Res*. 2021; 117(4):1078-1090. [CrossRef]
24. Li N, Liu JY, Timofeyev V, et al. Beneficial effects of soluble epoxide hydrolase inhibitors in myocardial infarction model: insight gained using metabolomic approaches. *J Mol Cell Cardiol*. 2009;47(6):835-845. [CrossRef]
25. Nivala M, Song Z, Weiss JN, Qu Z. T-tubule disruption promotes calcium alternans in failing ventricular myocytes: mechanistic insights from computational modeling. *J Mol Cell Cardiol*. 2015;79:32-41. [CrossRef]
26. Cutler MJ, Rosenbaum DS, Dunlap ME. Structural and electrical remodeling as therapeutic targets in heart failure. *J Electrocardiol*. 2007;40(6)(suppl):S1-S7. [CrossRef]
27. Lambert V, Capderou A, Le Bret E, et al. Right ventricular failure secondary to chronic overload in congenital heart disease: an experimental model for therapeutic innovation. *J Thorac Cardiovasc Surg*. 139(5):1197-1204. [CrossRef]
28. Lee JK, Kodama I, Honjo H, Anno T, Kamiya K, Toyama J. Stage-dependent changes in membrane currents in rats with monocrotaline-induced right ventricular hypertrophy. *Am J Physiol*. 1997;272(6 Pt 2):H2833-H2842. [CrossRef]
29. Helbing WA, Roest AA, Niezen RA, et al. ECG predictors of ventricular arrhythmias and biventricular size and wall mass in tetralogy of Fallot with pulmonary regurgitation. *Heart*. 2002; 88(5):515-519. [CrossRef]
30. Song J, Gao E, Wang J, et al. Constitutive overexpression of phosphomimetic phospholemman S68E mutant results in arrhythmias, early mortality, and heart failure: potential involvement of Na+/Ca2+ exchanger. *Am J Physiol Heart Circ Physiol*. 2012;302(3):H770-H781. [CrossRef]
31. Satoh H. Taurine modulates I(Kr) but I(Ks) in guinea-pig ventricular cardiomyocytes. *Br J Pharmacol*. 1999;126(1):87-92. [CrossRef]
32. Zhou Y, Xu W, Han R, et al. Matrine inhibits pacing induced atrial fibrillation by modulating I(km3) and I(Ca–L)[J]. *Int J Biol Sci*. 2012;8(1):150-158. [CrossRef]
33. Qu J, Volpicelli FM, Garcia LI, et al. Gap junction remodeling and spironolactone-dependent reverse remodeling in the hypertrophied heart. *Circ Res*. 2009;104(3):365-371. [CrossRef]
34. Gonzalez JP, Ramachandran J, Xie LH, Contreras JE, Fraidenraich D. Selective connexin43 inhibition prevents isoproterenol-induced arrhythmias and lethality in muscular dystrophy mice. *Sci Rep*. 2015;5(1):13490. [CrossRef]
35. Han XJ, Chen M, Hong T, et al. Lentivirus-mediated RNAi knockdown of the Gap junction protein, Cx43, attenuates the development of vascular restenosis following balloon injury. *Int J Mol Med*. 2015;35(4):885-892. [CrossRef]
36. Maesen B, Verheule S, Zeemering S, et al. Endomysial fibrosis, rather than overall connective tissue content, is the main determinant of conduction disturbances in human atrial fibrillation. *Europace*. 2022;24(6):1015-1024. [CrossRef]
37. Smyth JW, Hong TT, Gao D, et al. Limited forward trafficking of connexin 43 reduces cell-cell coupling in stressed human and mouse myocardium. *J Clin Invest*. 2010;120(1):266-279. [CrossRef]
38. Dhein S, Salameh A. Remodeling of cardiac gap junctional cell-cell coupling. *Cells*. 2021;10(9):2422. [CrossRef]
39. Leo-Macias A, Agullo-Pascual E, Delmar M. The cardiac connexome: non-canonical functions of connexin43 and their role in cardiac arrhythmias. *Semin Cell Dev Biol*. 2016;50:13-21. [CrossRef]
40. Mayyas F, Sakurai S, Ram R, et al. Dietary ω3 fatty acids modulate the substrate for post-operative atrial fibrillation in a canine cardiac surgery model. *Cardiovasc Res*. 2011;89(4):852-861. [CrossRef]
41. Akar FG, Nass RD, Hahn S, et al. Dynamic changes in conduction velocity and gap junction properties during development of pacing-induced heart failure. *Am J Physiol Heart Circ Physiol*. 2007;293(2):H1223-H1230. [CrossRef]
42. Hesketh GG, Shah MH, Halperin VL, et al. Ultrastructure and regulation of lateralized connexin43 in the failing heart. *Circ Res*. 2010;106(6):1153-1163. [CrossRef]
43. Agullo-Pascual E, Lin X, Leo-Macias A, et al. Super-resolution imaging reveals that loss of the C-terminus of connexin43 limits microtubule plus-end capture and NaV1.5 localization at the intercalated disc. *Cardiovasc Res*. 2014;104(2):371-381. [CrossRef]
44. Ning B, Zhang F, Song X, et al. Cardiac contractility modulation attenuates structural and electrical remodeling in a chronic heart failure rabbit model. *J Int Med Res*. 2020;48(10): 030006052096291. [CrossRef]
45. Lillo MA, Himelman E, Shirokova N, Xie LH, Fraidenraich D, Contreras JE. S-nitrosylation of connexin43 hemichannels elicits cardiac stress–induced arrhythmias in Duchenne muscular dystrophy mice. *JCI Insight*. 2019;4(24):130091. [CrossRef]
46. Shaw RM, Fay AJ, Puthenveedu MA, von Zastrow M, Jan YN, Jan LY. Microtubule plus-end-tracking proteins target gap junctions directly from the cell interior to adherens junctions. *Cell*. 2007;128(3):547-560. [CrossRef]
47. Li J, Li C, Liang D, et al. LRP6 acts as a scaffold protein in cardiac gap junction assembly. *Nat Commun*. 2016;7:11775. [CrossRef]
48. Brand-Schieber E, Werner P, Iacobas DA, et al. Connexin43, the major Gap junction protein of astrocytes, is down-regulated in inflamed white matter in an animal model of multiple sclerosis. *J Neurosci Res*. 2005;80(6):798-808. [CrossRef]
49. Poller W, Haas J, Klingel K, et al. Familial recurrent myocarditis triggered by exercise in patients with a truncating variant of the desmoplakin gene. *J Am Heart Assoc*. 2020;9(10):e015289. [CrossRef]
50. Lauf U, Giepmans BN, Lopez P, Braconnot S, Chen SC, Falk MM. Dynamic trafficking and delivery of connexons to the plasma membrane and accretion to gap junctions in living cells. *Proc Natl Acad Sci U S A*. 2002;99(16):10446-10451. [CrossRef]
51. dos Santos DO, Blefari V, Prado FP, et al. Reduced expression of adherens and gap junction proteins can have a fundamental role in the development of heart failure following cardiac hypertrophy in rats. *Exp Mol Pathol*. 2016;100(1):167-176. [CrossRef]
52. Brodehl A, Belke DD, Garnett L, et al. Transgenic mice overexpressing desmocollin-2 (DSC2) develop cardiomyopathy associated with myocardial inflammation and fibrotic remodeling. *PLOS ONE*. 2017;12(3):e0174019. [CrossRef]
53. Zhou Q, Zhou X, TuEr-Hong ZL, et al. Renal sympathetic denervation suppresses atrial fibrillation induced by acute atrial ischemia/infarction through inhibition of cardiac sympathetic activity. *Int J Cardiol*. 2016;203:187-195.[CrossRef]